Nuclear Engineering and Technology 54 (2022) 867–876

Contents lists available at ScienceDirect

Nuclear Engineering and Technology

journal homepage: www.elsevier.com/locate/net

Original article

Experimental study on heat transfer characteristics of supercritical carbon dioxide natural circulation

Pengfei Wang [a], Peng Ding [b], Wenhuai Li [b], Rongshun Xie [a], Chengjie Duan [b], Gang Hong [a, c], Yaoli Zhang [a, c, *]

[a] College of Energy, Xiamen University, Xiamen, Fujian, 361105, China
[b] China Nuclear Power Technology Research Institute Co. Ltd, Shenzhen, Guangdong, 518028, China
[c] Fujian Research Center for Nuclear Engineering, Xiamen, Fujian, 361105, China

ARTICLE INFO

Article history:
Received 15 April 2021
Received in revised form
25 August 2021
Accepted 26 August 2021
Available online 1 September 2021

Keywords:
Supercritical carbon dioxide
Buoyancy
Heat transfer correlation
Bulk flow acceleration
Horizontal flow

ABSTRACT

An experimental study has been conducted to investigate the heat transfer characteristics of supercritical carbon dioxide (sCO_2) uniformly heated in the horizontal circular smooth tube. The results illustrated that there was a significant difference in heat transfer between the top wall and bottom wall due to the buoyancy. Bulk flow acceleration cannot be negligible in the high heat flux region, which leads to heat transfer deterioration. A new heat transfer correlation is proposed, in which the buoyancy parameter and bulk flow acceleration have been taken into account. The new correlation and six classic correlations for sCO_2 are examined in horizontal tubes. The comparison indicates that the new correlation has a better performance for sCO_2 flowing through a horizontal heating tube under natural circulation conditions. For example, 94.9% of the calculated results using the new heat transfer correlation were within ±30% of the experimental results while only 87.9% of that using the Jackson correlation (the best of the six) were within the same error bands.

1. Introduction

Carbon dioxide is inexpensive, environmentally-friendly, abundant in reserves, and has moderate critical conditions. The critical pressure and temperature are 7.38 MPa and 31.26 °C, respectively. Because of the outstanding thermodynamic characteristics, supercritical carbon dioxide (sCO_2) is regarded as the most attractive working fluid for GEN IV nuclear reactors. For example, the Brayton cycle with sCO_2 as working fluid can not only effectively improve the thermal efficiency of lead-cooled or sodium-cooled fast reactors, but also significantly reduce the size and the power consumption, making the cycle system more compact [1]. The widespread use of sCO_2 in the field of nuclear energy is of great significance to the optimization of nuclear power systems and the rapid development of the nuclear industry.

The heat transfer characteristics of sCO_2 heated in tubes are very important for the design and optimization of industrial energy conversion systems. However, in the pseudo-critical region, the physical properties of sCO_2 exhibit extremely rapid variations with the temperature, as shown in Fig. 1, which makes the heat transfer characteristics more complex. Therefore, in recent years, a number of researchers have investigated the heat transfer performances of sCO_2 in tubes. Kim et al. [2] carried out convection heat transfer experiment of sCO_2. The heat transfer correlation of vertical heating tube was obtained by using piecewise function correction and considering the buoyancy factor. Bae et al. [3] investigated the effects of buoyancy and bulk flow acceleration on the heat transfer of vertical tube. They believed that it was necessary to develop corresponding correlations for normal heat transfer and heat transfer deterioration, in order to improve the accuracy of calculations. Based on experimental data and theoretical analysis, Kim et al. [4] developed a different type of the heat transfer model for vertical tube. Liu et al. [5,6] evaluated typical heat transfer correlations based on the published experimental data of sCO_2 forced convection heat transfer. They found that the calculation results of the existing heat transfer correlations were quite different from the experimental results, in the pseudo-critical region. The ambiguous heat transfer mechanism, imperfect mathematical model, and limited measurement accuracy are the main reasons for the poor prediction results of heat transfer correlations. Zhang et al. [7]

* Corresponding author. College of Energy, Xiamen University, Xiamen, Fujian, 361105, China.
E-mail address: zhangyl@xmu.edu.cn (Y. Zhang).

https://doi.org/10.1016/j.net.2021.08.031

Nomenclature

c_p	specific heat, J/kg·K
U	voltage from the DC power supply, V
I	current from the DC power supply, A
R_{el}	electrical resistance, Ohm
Q	heat transfer rate, W
G_m	mass flow rate, kg/s
h	specific enthalpy, J/kg
r	radius, m
l	heated length, m
q	heat flux, W/m^2
D	diameter, m
T	temperature, K
P	pressure, Pa
q_v	volumetric heat generation, W/m^3
x	axial location in the flow direction, m
HTC	convective heat transfer coefficient, W/m^2 K
g	acceleration of gravity, m/s^2
G	mass flux, kg/m^{2}s
A	Inner surface area of heating section, m^2

Greek Symbols

ρ	density, kg/m^3
λ	thermal conductivity, W/m·K
ν	kinetic viscosity, m^2/s
μ	dynamic viscosity, Pa·s
β	thermal expansion coefficient, 1/K

Dimensionless

Nu	Nusselt number; $(\frac{HTC\times D_i}{\lambda})$
f	friction factor
Re	Reynolds number; $(\frac{GD_i}{\mu})$
Pr	Prandtl number; $(\frac{\mu c_p}{\lambda})$
Bu$_c$	buoyancy parameter; $(\mathbf{Gr}_b\mathbf{Re}_b^{-2})$
Gr	Grashof number; $(\frac{g\beta(Tw_{in}-T_b)D_i^3}{\nu^2})$
q$^+$	bulk flow acceleration; $(\frac{q\beta_b}{Gc_{p,b}})$

Subscripts

pc	pseudo-critical point
in	inlet
out	outer
i	inner
o	external
b	bulk
w	wall
exp	experimental data
cal	calculated data

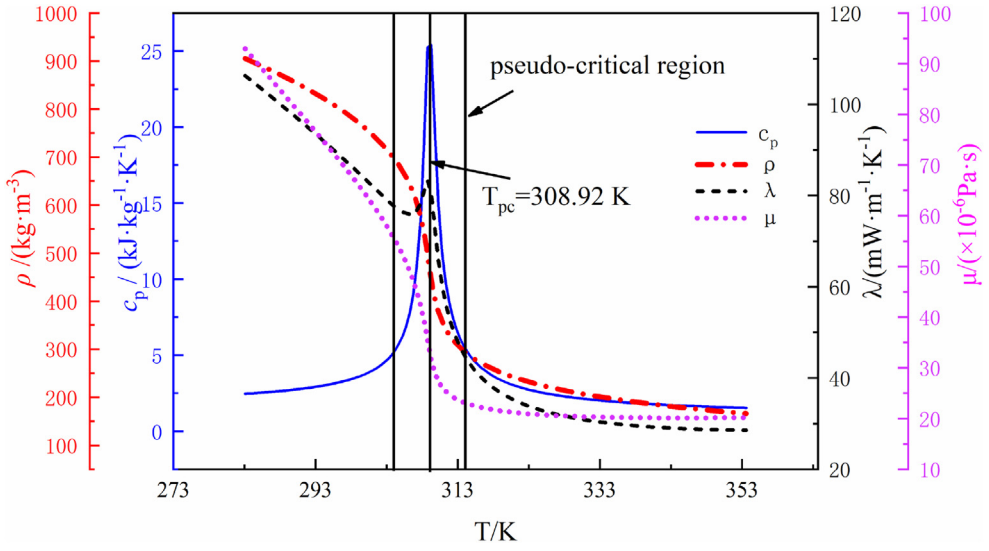

Fig. 1. Variation of thermal and transport properties of CO_2 at 8.2 MPa.

studied experimentally convection heat transfer of sCO_2 in a vertical heating tube. They found that there are significant differences in the heat transfer characteristics under various mass flow rates. Based on the experimental data, a model was established for vertical heating tubes. Zhang et al. [8] proposed the supercritical-boiling- number to judge the transition boundary between the normal heat transfer and heat transfer deterioration of sCO_2 in a vertical tube. In the case of the horizontal flow, since buoyancy appears in the perpendicular direction of the flow, heat transfer characteristics are more complicated than that in the vertical flow, which results in a non-uniform temperature distribution in the circumferential direction. Therefore, many conclusions obtained on vertical pipes are not applicable to horizontal pipes. Zhao et al. [9] experimentally studied heat transfer coefficients from sCO_2 flowing in horizontal mini/micro channels. They found that although sCO_2 was in forced motion through the horizontal tubes at Reynolds numbers up to 10^5, the buoyancy effect was still significant. Then, a correlation was developed for the axially averaged Nusselt number in terms of buoyancy parameters for forced convection of sCO_2 in horizontal mini/micro tubes. Tanimizu and Sadr [10] compared three commonly used buoyancy parameters including **Bu$_c$**, **Bu$_J$** and **Bu$_p$** in the heated horizontal tube. They deemed that **Bu$_c$** was the best prediction of the buoyancy effect among three parameters. Wang et al. [11] used the experimental data of Adebiyi and Hall [12] to simulate the flow of sCO_2 in a horizontally heated circular tube. The simulation results showed that secondary circulation caused by

buoyancy will influence the flow structure and turbulence levels. For large horizontal tubes, the heat transfer is slightly enhanced near the pseudocritical point, but the heat transfer deteriorates significantly at higher heat fluxes. This result is contrary to the results of small-diameter tubes published in the past. Zhan et al. [13]numerically studied the asymmetric heat transfer characteristics of sCO_2 in a horizontal tube considering buoyancy parameter.

It should be pointed out that many of the heat transfer characteristics of sCO_2 are explored under vertical heating tubes, and these results cannot be directly used in horizontal heating tubes. Moreover, many scholars have fitted some heat transfer correlations considering different factors, and these correlations need to be compared. Most of all, the current research focuses on the heat transfer characteristics of sCO_2 under forced circulation, while there are relatively few researches on natural flow under horizontal heating condition. Especially, there is almost no specific heat transfer correlation for sCO_2 flowing through a horizontal heating tube under natural circulation conditions.

In this study, an experimental system was established to investigate the heat transfer characteristics of sCO_2 heated in a horizontal tube. The effects of buoyancy and bulk flow acceleration on the heat transfer coefficient were examined. Based on the experimental data, a new heat transfer correlation was derived. Compared with other correlations in published literatures, the new correlation stands out as the better choice for the scenarios involving natural sCO_2 tube flow under heating conditions. This study can provide a reference for the heat transfer design of an energy conversion system using sCO_2 as working fluid.

2. Experimental facility and method

2.1. Experimental loop

An experimental system was designed and constructed to quantify the heat transfer in sCO_2 horizontal flow as depicted in Fig. 2. The main facilities include vacuum pump, Coriolis force mass flowmeter, CO_2 tank, water cooling machine, pressurizer, differential pressure transmitter, pressure transmitter, T-type thermocouple, etc. According to different functions, the system can be divided into six subsystems. (1) Vacuum subsystem: Before the experiment, the non-condensable gas in the gas supply system, the primary circuit and all related pipelines was purged “completely” by long operation of the vacuum pump. (2) CO_2 gas supply subsystem: The gas supply system is turned on to allow gaseous carbon dioxide in the CO_2 tank to enter at about 7 MPa. In the gas supply subsystem, the gas is first liquidized by cooling. The liquid is then compressed by the plunger pump to the working pressure, up on which it is injected into the primary circuit. (3) Cooling water subsystem: The water cooling machine provides a stable cold source, and the heat is continuously taken out of the experimental loop through the double-pipe heat exchanger. (4) Heating subsystem of the horizontal experimental section: The positive and negative terminals of the DC power supply are clamped at both ends of the heating section tube to heat the test section. (5) Stable pressure control subsystem: In the primary circuit, the pressurizer is used to suppress the pressure fluctuations while the back-pressure valve is used to prevent the loop pressure go higher than the working pressure. When that happens, the backpressure valve will open to release the excessive carbon dioxide liquid and bring the loop pressure back to the desired level. (6) Data acquisition and display subsystem: Sensors collect measurement signals. Then these signals are processed, displayed and saved in real time by computer. The six subsystems make sCO_2 flow stably in the rectangular loop. The circulation loop has no external power equipment, such as pumps, compressors, etc., and is driven entirely by the density difference between the cold and hot fluids. Therefore, this is a natural circulation.

The primary circuit is a regular rectangular structure, the length and height are 4.35 m and 2.65 m respectively. The specific positions and geometric parameters of each equipment in the experimental bench are shown in Fig. 3.

2.2. Layout of the test section

The experimental section is made of 316L stainless steel pipe with a total length of 3350 mm. The length of heated section is

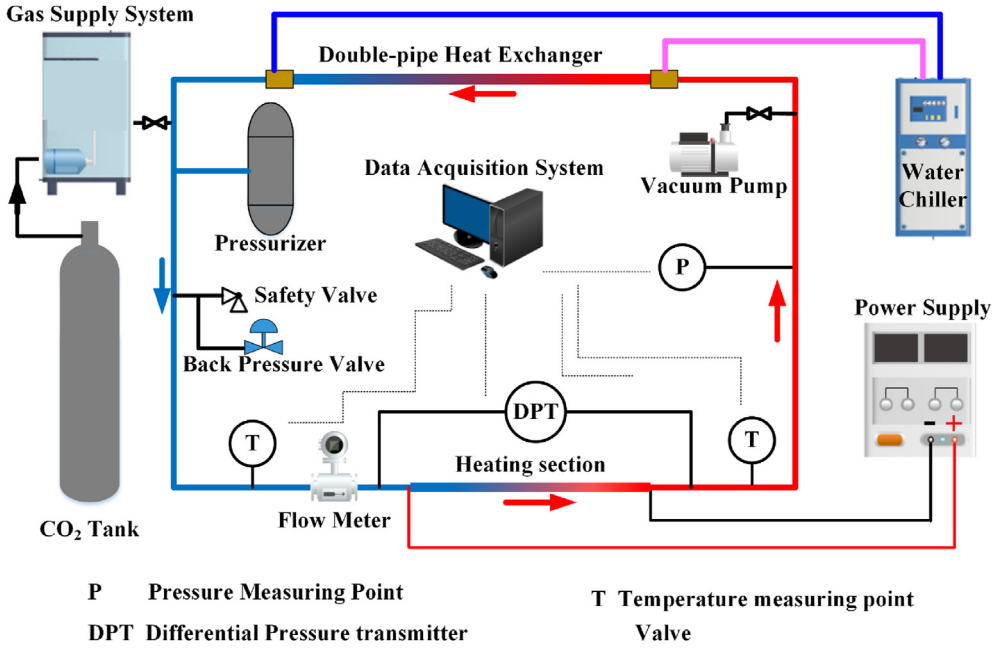

Fig. 2. Schematic diagram of the experimental loop.

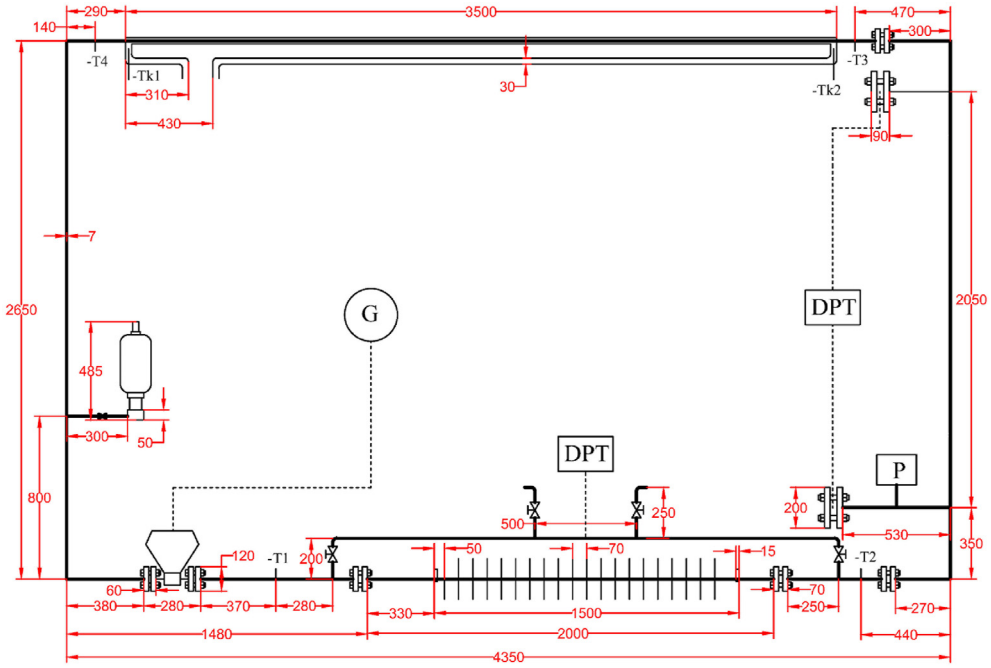

Fig. 3. The geometry of the experimental facility.

1500 mm, and there are two adiabatic sections with 160 mm and 700 mm, respectively, as a developing section. The inner diameter and thickness of tube are 7 mm and 1.5 mm, respectively. Two electric insulation flanges are set at the two ends of the experimental section. The structure of the experimental section and the arrangement of temperature measurement points are shown in Fig. 4. The pipeline between the two copper electrodes is the effective heating length, and 20 equidistant sections are set on it. The first thermocouple section is 50 mm away from the positive terminal, and the negative terminal is 120 mm away from the last thermocouple section. A thermocouple is arranged at top and bottom of each section, a total of 40 wall temperature measuring points. The experiment section is wrapped with two materials of 50 mm thick high-temperature and fire-resistant ceramic fiber cotton and aluminum foil glass wool roll felt for double insulation, reducing the heat loss of the experiment section.

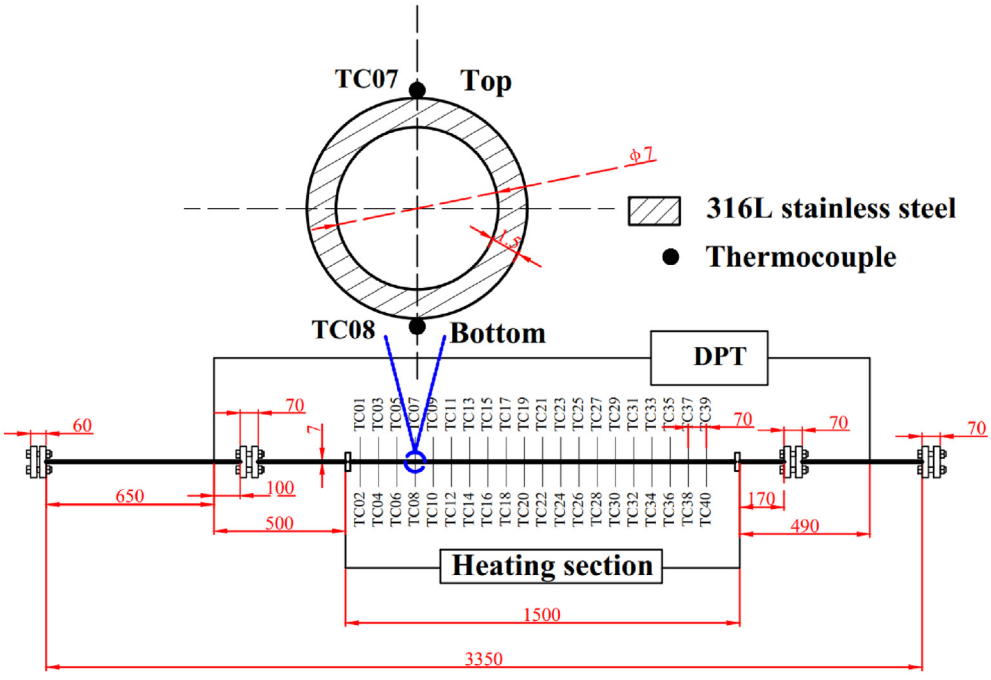

Fig. 4. Schematic of the test section.

3. Data reduction and uncertainty analysis

3.1. Data reduction

The experimental data was reduced to calculate local heat transfer coefficients as a following procedure. The output power of the power supply is calculated as

$$Q_{total} = UI = I^2 R_{el} \tag{1}$$

Where U is the voltage imposed on the test section, I is the current, R_{el} is the resistance of the heating section.

The heat transfer rate Q from CO_2 to the tube wall can be obtained from the energy balance under a steady state:

$$Q = G_m\left(h_{f,out} - h_{f,in}\right) \tag{2}$$

Where G_m is the mass flow rate, $h_{f,in}$ and $h_{f,out}$ are the enthalpies at the inlet and outlet of the test section, which are obtained from the relevant look-up table in the NIST REFPROP library [14] given the temperatures and pressures of the two locations.

The experimental section is uniformly heated and the heat flux q_w can be evaluated as:

$$q_w = \frac{Q}{2\pi r_i l} \tag{3}$$

The heat loss in the heating section can be calculated as

$$Q_{loss} = Q_{total} - Q \tag{4}$$

The heat flux loss is expressed into Eq. (5).

$$q_{loss} = \frac{Q_{loss}}{2\pi r_o l} \tag{5}$$

Where l is the effective heated long , r_i and r_o is the inner radius and outer radius of test section.

The heating efficiency can be calculated by Eq. (6)

$$\eta = \frac{Q_{loss}}{Q_{total}} \tag{6}$$

The results of the data show that the heating efficiency can reach more than 93%, indicating that the heat insulation effect is great and meets the experimental requirements.

The equivalent internal heat source generated by the resistance of the experimental section is:

$$q_v = \frac{4Q_{total}}{\pi\left(D_o^2 - D_i^2\right)L_h} = \frac{Q_{total}}{\pi\left(r_o^2 - r_i^2\right)l} \tag{7}$$

The temperature of the outer wall is measured in the experiment, and the temperature of the inner wall needs to be derived. Eqs. (8) and (9) show the one-dimensional heat-conduction equation and the boundary conditions.

$$\frac{1}{r}\frac{d}{dr}\left(r\lambda\frac{dT}{dr}\right) + q_v = 0 \tag{8}$$

$$\begin{cases} -\lambda\left.\dfrac{dT}{dr}\right|_{r=r_o} = q_{loss} \\ T(r_o) = T_{w,out} \end{cases} \tag{9}$$

The local inner wall temperature ($T_{w,in}$) can be evaluated as:

$$T_{w,in} = T_{w,out} - \frac{q_v}{4\lambda}\left(r_i^2 - r_o^2\right) + \frac{r_o}{\lambda}\left(\frac{q_v r_o}{2} - q_{loss}\right)\ln\frac{r_i}{r_o} \tag{10}$$

Where λ is the thermal conductivity of the experimental section.

The heating section is a boundary condition of uniform heat flux. According to the energy balance equation, the local fluid bulk enthalpy is calculated by:

$$h_{b,x} = h_{in} + \frac{Q}{G_m}\frac{x}{l} \tag{11}$$

With the local specific enthalpy value and pressure known, local fluid temperature $T_{b,i}$ can be obtained from NIST REFPROP library. Then, local heat transfer coefficient is calculated from:

$$HTC = \frac{q_w}{T_{w,i} - T_{b,i}} \tag{12}$$

The Nusselt number obtained by the experiment is:

$$Nu_{\exp} = \frac{HTC \times D_i}{\lambda_b} \tag{13}$$

where λ_b is the thermal conductivity of the fluid and D_i is the inner diameter.

In order to analyze heat transfer enhancement or heat transfer deterioration, Kim et al. [15] believed that when the ratio (**Nu***) of **Nu** obtained from the experiment to **Nu** calculated by the Gnielinski [16] correlation is greater than 1, the heat transfer is enhanced. When the **Nu*** is less than 1, heat exchange deteriorates.

$$\mathbf{Nu_{Gnielinski}} = \frac{(\mathbf{f}/8)(\mathbf{Re_b} - 1000)\mathbf{Pr_b}}{1 + 12.7\sqrt{\mathbf{f}/8}\left(\mathbf{Pr_b}^{2/3} - 1\right)}\left[1 + \left(\frac{d}{l}\right)^{2/3}\right]\left(\frac{T_b}{T_w}\right)^{0.45} \tag{14}$$

$$\mathbf{Nu}^* = \frac{\mathbf{Nu_{exp}}}{\mathbf{Nu_{Gnielinski}}} \tag{15}$$

3.2. Uncertainty analysis

If an indirect measurement is composed of a number of direct measurements, that is, $R = f_{(x1,x2,\ldots,xn)}$, then the uncertainty of this indirect measurement is defined by the expression from Moffat [17] as follows.

$$\Delta R = \sqrt{\left(\frac{\partial R}{\partial x_1}\Delta x_1\right)^2 + \left(\frac{\partial R}{\partial x_2}\Delta x_2\right)^2 + \cdots\cdots + \left(\frac{\partial R}{\partial x_n}\Delta x_n\right)^2} \tag{16}$$

The calculation formulas for the uncertainty of q, h and **Nu** are as follows:

$$\frac{\delta q}{q} = \sqrt{\left(\frac{\delta Q}{Q}\right)^2 + \left(\frac{\delta A}{A}\right)^2} \tag{17}$$

$$\frac{\delta h}{h} = \sqrt{\left(\frac{\delta q}{q}\right)^2 + \left(\frac{\delta A}{A}\right)^2 + \left(\frac{\delta T}{T_{w,in} - T_b}\right)^2} \tag{18}$$

$$\frac{\delta \mathbf{Nu}}{\mathbf{Nu}} = \sqrt{\left(\frac{\delta h}{h}\right) + \left(\frac{\delta \lambda}{\lambda}\right) + \left(\frac{\delta d}{d}\right)} \tag{19}$$

Table 1
Uncertainties of the main experimental parameters.

Parameters	Units	Uncertainties (%)
Temperature	K	±0.41%
Pressure	Pa	±0.12%
Mass flow rate	kg/s	±0.1%
Heating power	W	±3.42%
Heat flux	W/m^2	±3.85%
Convective heat transfer coefficient	W/(m^2·K)	±4.26%
Nu	/	±4.29%

Table 1 below shows the uncertainty of the relevant measured and calculated quantities.

4. Experimental results and discussion

4.1. Heat transfer characteristics

Under all experimental conditions, the top wall temperature of the same heating section is higher than the bottom wall temperature. Fig. 5 shows the distribution of wall temperature at different positions of the experimental section. It can be found that when the pressure is 9.2 MPa and the heat flux is 132.35 kW/m^2, the maximum temperature difference between the top wall and the bottom wall can reach 33.4 K. For the bulk temperature, it increases gradually at the beginning, changes little near the pseudo-critical temperature, and increases again after passing the pseudo-critical region. This is because the specific heat capacity of sCO_2 first increases and then decreases with the increase of temperature. In the pseudo-critical region, the specific heat capacity is larger and the fluid has a stronger ability to absorb heat. However, when the bulk temperature exceeds the pseudo-critical temperature, the specific heat capacity has dropped to a lower level. Such a large heat flux can only remove the heat in the form of increasing the temperature difference, which shows the wall temperature soaring. Fig. 6 shows the distribution of heat transfer coefficient at different positions of the experimental section. It can be found that the fluid has obvious heat transfer enhancement in the pseudo-critical region, and the heat transfer coefficient is larger.

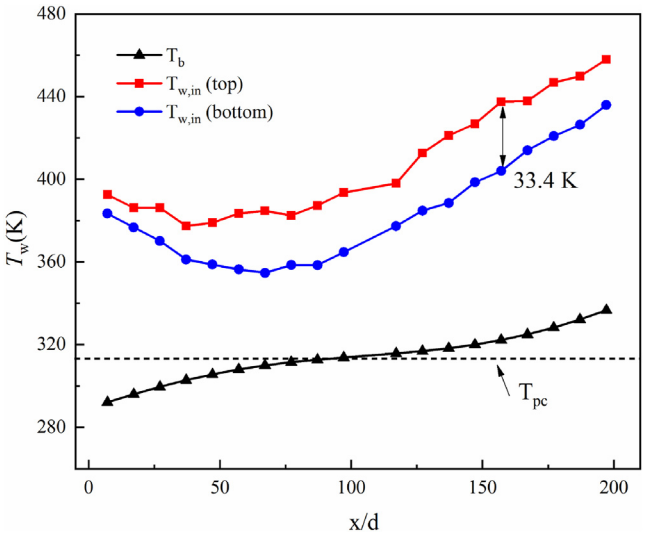

Fig. 5. Distribution of wall temperature when P = 9.2 MPa and q = 132.35 kW/m.^{2}.

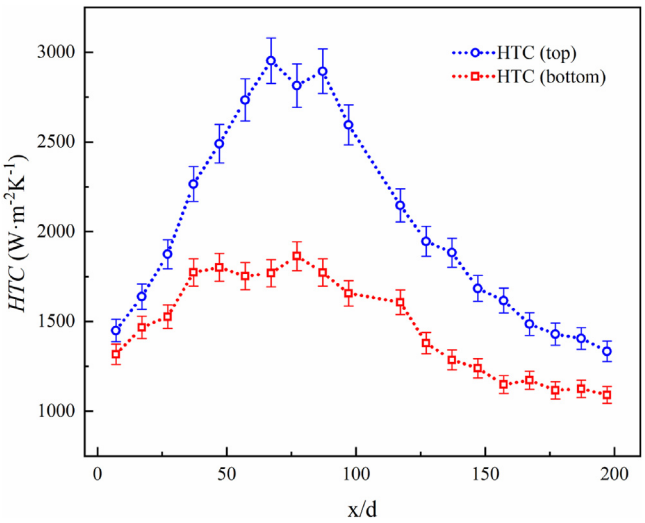

Fig. 6. Heat transfer coefficient at different positions when P = 9.2 MPa and q = 132.35 kW/m.^{2}.

4.2. Effect of buoyancy and bulk flow acceleration

When sCO_2 flows through the heated horizontal tube, the temperature field distribution on the section is uneven due to the buoyancy effect, making the top wall temperature of the same section higher than the bottom wall temperature. Jackson et al. [18] summarized the dimensionless number of buoyancy on the heat transfer of horizontal tubes. They believe that when $\mathbf{Bu_c} < 10^{-3}$, the effect of buoyancy can be negligible.

$$\mathbf{bu_C} = \mathbf{Gr_b Re_b^{-2}} \tag{20}$$

Regarding the effect of bulk flow acceleration on the heat transfer in the heated horizontal tube, many scholars [2–4,19,20] used the dimensionless factor $\mathbf{q}^+$ to characterize the strength of bulk flow acceleration in the experiment. It is considered that when $\mathbf{q}^+ \leq 5 \times 10^4$, the bulk flow acceleration can be ignored.

$$\mathbf{q}^+ = \frac{q\beta_\mathbf{b}}{Gc_{p,b}} \tag{21}$$

where β_b is the thermal expansion coefficient of the fluid and G is the mass flux.

When q < 40 kW/m^2, it is a low heat flux area, when 40 kW/m^2 < q < 80 kW/m^2 is a medium heat flux area, and when q > 80 kW/m^2, it is a high heat flux area.

Fig. 7 and Fig. 8 show the changes in the buoyancy parameter and bulk flow acceleration of the top wall temperature and bottom wall temperature in different heat flux areas along the flow direction. It can be seen that $\mathbf{Bu_c}$ is far greater than the threshold 10^{-3} under all experimental conditions, which indicates that buoyancy always exists and significantly affects the heat transfer of the sCO_2. In the low heat flux area, the heat transfer deterioration of the top wall is not obvious, and **Nu*** is around 0.9. When in the region of high heat flux, $\mathbf{Bu_c}$ drops rapidly, at this time bulk flow acceleration has a greater impact on heat transfer. It can be seen that both the top wall and the bottom wall will have heat transfer deterioration, but the heat transfer coefficient of the bottom wall is always higher than that of the top wall. Due to buoyancy, flow stratification occurs in the pipe flow. The density difference induces a secondary flow, transporting the heated fluid to the top of the tube. As a result,

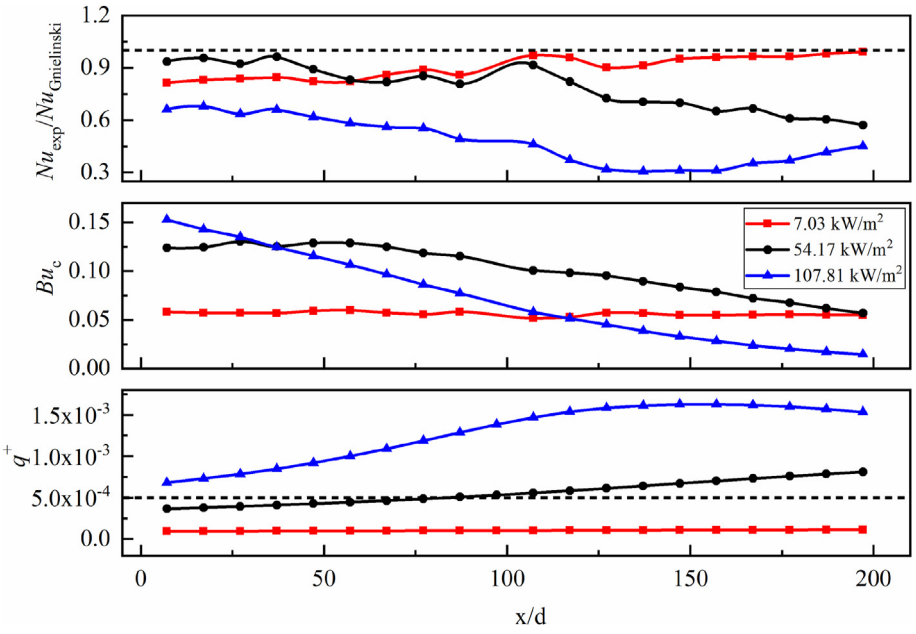

Fig. 7. Buoyancy parameter and bulk flow acceleration for the top wall at different heat fluxes.

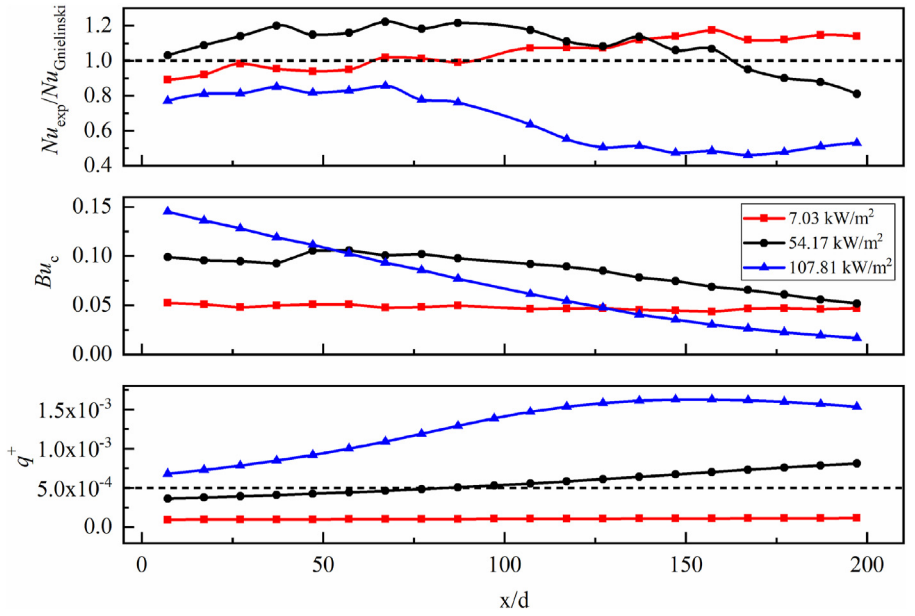

Fig. 8. Buoyancy parameter and bulk flow acceleration for the bottom wall at different heat fluxes.

high-temperature with low density is accumulated at the top, making the top wall temperature higher than the bottom wall temperature. For bulk flow acceleration, it can be found that in the low heat flux area, $\mathbf{q}^+$ is much smaller than the threshold, and the effect of bulk flow acceleration can be negligible. The **Nu*** is close to 1, and the heat transfer is normal. When in the high heat flux area, $\mathbf{q}^+$ is greater than 5×10^{-4} in the experimental section, the effect of bulk flow acceleration is prominent, and the heat transfer has also been significantly deteriorated. As shown in the figure, when the heat flux is 107.81 kW/m^2, **Nu*** is only about 0.6 at this time, and the heat transfer is deteriorated. The bulk flow acceleration will cause the fluid flow to re-laminar fluidization, leading to deterioration of heat transfer. All in all, that the bulk flow acceleration has little effect on the heat transfer of sCO_2 when the heat flow density is low, but when the heat flow density is high, it will worsen the heat transfer of the fluid. It can be seen that the buoyancy and bulk flow acceleration have an important influence on the heat transfer of the natural circulation horizontal tube. Therefore, these two factors should be considered in the correlation of convective heat transfer under natural circulation conditions.

4.3. Assessments of heat transfer correlations for sCO_2

So far, the heat transfer empirical correlation is still the most

Table 2
Heat transfer empirical correlations.

Author	Correlation	Flow direction
Dittus-Boelter [21]	$\mathbf{NuD}-\mathrm{B}=0.023\mathbf{Re_b^{0.8}Pr_b^{0.4}}$	Horizontal/Vertical
Petukhov-Kirillov [22]	$\mathbf{NuP}-\mathrm{K}=\frac{(\mathbf{f}/8)\mathbf{Re_b Pr_b}}{1.07+12.7\sqrt{\mathbf{f}/8}(\mathbf{Pr_b^{2/3}}-1)}$ $\mathbf{f}=(1.82\lg\mathbf{Re_b}-1.64)^{-2}$	Horizontal/Vertical
Gnielinski [16]	$\mathbf{Nu_{Gnielinski}}=\frac{(\mathbf{f}/8)(\mathbf{Re_b}-1000)\mathbf{Pr_b}}{1+12.7\sqrt{\mathbf{f}/8}(\mathbf{Pr_b^{2/3}}-1)}\left[1+\left(\frac{d}{l}\right)^{2/3}\right]\left(\frac{T_b}{T_w}\right)^{0.45}$	Horizontal/Vertical
Jackson [23]	$\mathbf{Nu_{Jackson}}=0.0183\mathbf{Re_b^{0.82}Pr_b^{0.5}}\left(\frac{\rho_w}{\rho_b}\right)^{0.3}\left(\frac{\overline{c_p}}{c_{p,b}}\right)^{n}$ $\begin{cases} n=0.4 \quad , T_b<T_w<T_{pc} \text{ or } 1.2T_{pc}<T_b<T \\ n=0.4+0.2\left(\frac{T_w}{T_{pc}}-1\right) \quad , T_b<T_{pc}<T_w \\ n=0.4+0.2\left(\frac{T_w}{T_{pc}}-1\right)\left[1-5\left(\frac{T_b}{T_{pc}}-1\right)\right] \quad , T_{pc}<T_b<1.2T_{pc},\ T_b<T_w \end{cases}$	Horizontal/Vertical
Zhao [9]	$\mathbf{Nu_{Zhao}}=0.124\mathbf{Re_b^{0.8}Pr_b^{0.4}}\left(\frac{\mathbf{Gr}}{\mathbf{Re_b^2}}\right)^{0.203}\left(\frac{\rho_w}{\rho_b}\right)^{0.842}\left(\frac{\overline{c}_p}{c_{p,b}}\right)^{0.384}$	Horizontal
Li [24]	$\mathbf{Nu_{Li}}=0.023\mathbf{Re_b^{0.8}Pr_b^{0.4}}\left(\frac{\rho_w}{\rho_b}\right)^{0.3}\left(\frac{\overline{c_p}}{c_{pb}}\right)^{n}$ $\begin{cases} n=0.4 \quad , T_b<T_w<T_{pc} \text{ or } 1.2T_{pc}<T_b<T \\ n=0.4+0.2\left(\frac{T_w}{T_{pc}}-1\right) \quad , T_b<T_{pc}<T_w \\ n=0.4+0.2\left(\frac{T_w}{T_{pc}}-1\right)\left[1-5\left(\frac{T_b}{T_{pc}}-1\right)\right] \quad , T_{pc}<T_b<1.2T_{pc},\ T_b<T_w \end{cases}$	Horizontal

important way to calculate the heat transfer of sCO_2. Some researchers have fitted the heat transfer correlations in horizontal heating tubes. Most of them use dimensionless numbers, such as **Pr** and **Re**, and fit the experimental data by adding fluid property correction terms. The common heat transfer correlations for horizontal tubes are listed in Table 2.

The following indicators are used to evaluate these heat transfer correlations.

The relative error of the heat transfer correlations is given by the following expression:

$$error=\frac{\mathbf{Nu_{exp}}-\mathbf{Nu_{cal}}}{\mathbf{Nu_{exp}}} \tag{22}$$

Where $\mathbf{Nu_{exp}}$ and $\mathbf{Nu_{cal}}$ are the experimental results and the calculation results of the heat transfer correlation, respectively.

If the error is less than 10%, record it as $E_{\pm 10}$ Therefore, the percentage within calculation error of each data can be obtained.

$$E_{\pm 10\%}, E_{\pm 20\%}, E_{\pm 30\%} \tag{23}$$

The mean absolute percentage error (*MAPE*) is defined as follows:

$$MAPE=\frac{1}{n}\sum_{i=1}^{n}|error|\times 100 \quad (\%) \tag{24}$$

Where n is the number of experimental points.

The standard deviation of the error (σ):

Table 3
Comparison of the experimental and predicted *Nu* using empirical correlations.

Correlation	$E_{\pm 10\%}$	$E_{\pm 20\%}$	$E_{\pm 30\%}$	MAPE%	σ
Zhao	0.5	1.4	3.2	90	45.8
Dittus-Boelter	18.2	34.3	48.1	61.7	96.3
Gnielinski	18.8	35.6	47.6	72.6	116.3
Petukhov-Kirillov	18.5	34.5	46.8	74.5	120.3
Li	39.8	67.2	86.6	16.1	12.9
Jackson	40.2	73.7	87.9	15.9	14.7

$$\sigma=\sqrt{\frac{\sum_{\mathbf{i}=1}^{n}\left(error\text{-}\overline{error}\right)^2}{n}}\times 100(\%) \tag{25}$$

A total of 12160 data are used for calculation. Table 3 shows the evaluation results of the heat transfer correlations. It can be found that the accuracy of Zhao correlation is poor under the large-diameter experimental conditions currently studied. Although the correlation is suitable for horizontal pipes, it is mainly used in the micro pipe diameter. In this experiment, large diameter pipe is used, so Zhao correlation is not suitable for this experiment. The calculation accuracy of the Dittus-Boelter, Gnielinski, and Petukhov-Kirillov heat transfer correlations is also poor, and the data whose calculation deviation is within ±30% account for less than 50%, indicating that these correlations cannot adapt to drastic changes in thermophysical properties. When calculating the heat transfer of sCO_2, these correlations should be corrected. Li and Jackson used thermophysical properties modification to optimize the heat transfer correlation. The calculation accuracy of these two

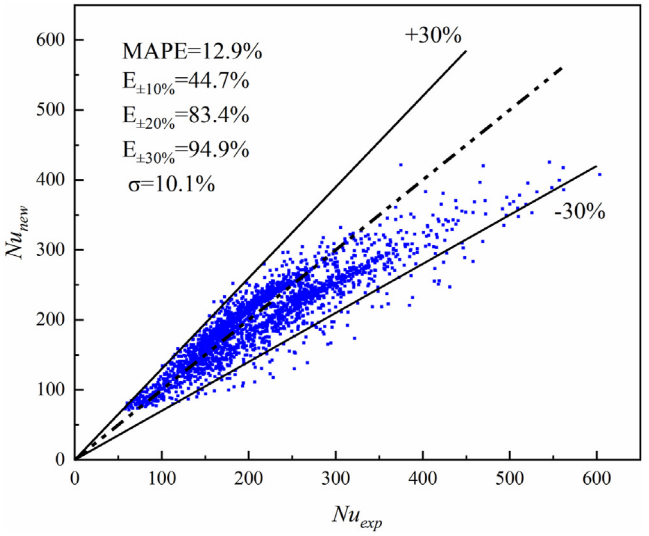

Fig. 9. Comparison between the experimental data and the calculated data based on the new correlation.

correlations is relatively good, the average absolute percentage error is about 16%, and the data with calculation deviation within ±30% accounts for about 87%. Both of these correlations take into account the influence of the specific heat capacity distribution in different temperature ranges on the convective heat transfer of sCO_2. Therefore, a piecewise function is used in the correction of the comparative heat capacity term.

4.4. A new heat transfer correlation for sCO_2

It can be seen that buoyancy effect, bulk flow acceleration and thermophysical properties have great influence on the heat transfer of horizontal heating tube. Combined with the previous research on the heat transfer correlation, considering the effect of various factors, a new heat transfer correlation is proposed based on experimental data.

$$\mathbf{Nu} = 0.0183\mathbf{Re_b^{0.82}Pr_b^{0.5}}\left(\frac{\lambda_w}{\lambda_b}\right)^{0.04}\left(\frac{\rho_w}{\rho_b}\right)^{0.3}\left(\frac{\overline{c_p}}{c_{p,b}}\right)^{n} e^{(\mathbf{bu}_\tau^{2.3})} e^{(\mathbf{q}^{+0.7})} \tag{26}$$

Where n is defined as:

$$\begin{cases} n = 0.52 \ , T_b < T_w < T_{pc} \text{ or } 1.2T_{pc} < T_b < T_w \\ n = 0.52 + 0.2\left(\dfrac{T_w}{T_{pc}} - 1\right) \ , T_b < T_{pc} < T_w \\ n = 0.52 + 0.2\left(\dfrac{T_w}{T_{pc}} - 1\right)\left[1 - 5\left(\dfrac{T_b}{T_{pc}} - 1\right)\right] \ , T_{pc} < T_b < 1.2T_{pc}, T_b < T_w \end{cases} \tag{27}$$

The new correlation is suitable for the calculation of the heat transfer of sCO2 in the horizontal heating tube under natural circulation conditions. The specific application range is: system pressure is 7.58–10.26 MPa, inlet temperature is 289.04–306.33 K, outlet temperature is 294.59–382.57 K, heat flux is 3.61–148.82 kW/m^2, mass flux is 189.45–514.46 kg/(m^2·s), outlet velocity is 0.23–2.65 m/s, outlet **Re** is 1.59×10^4–1.66×10^5, and **Pr** is 0.72–14.29.

Fig. 9 shows the comparison between the calculated results of the new correlation and the experimental results. There are a total of 12160 convective heat transfer data points in the experiment. In order to show in the figure, the sampling interval is set to 5, that is, 1 data is randomly selected from every 5 data. It can be seen that the calculation results of the new correlation are very close to the experimental results. Compared with the experimental data, the average absolute percentage error of the new heat transfer correlation is only 12.9%, the standard deviation is 10.1%, the calculation deviation of data within ±10% can account for 45%. The proportion of data whose calculation deviation is within ±30% is as high as 94.9%. The calculation accuracy of the new heat transfer correlation is the highest.

5. Conclusions

Experimenting with sCO_2 natural circulation allows to study the heat transfer characteristics of sCO_2 flowing in a uniformly heated horizontal tube. The effects of buoyancy and bulk flow acceleration are studied and discussed in detail. Based on the experimental data, a new heat transfer correlation is proposed, and six classic heat transfer correlations are evaluated in horizontal tube. The obtained conclusions are summarized as follow:

1. The buoyancy significantly affects the heat transfer, resulting in the difference between the top wall and the bottom wall. Bulk flow acceleration cannot be negligible in the high heat flux region, which leads to heat transfer deterioration.
2. Among the six classic heat transfer correlations, the Jackson correlation has a good calculation result, and the data whose calculation error is within ±30% accounts for 87.9%.
3. The new heat transfer correlation that takes into account the effects of buoyancy and bulk flow acceleration has the highest calculation accuracy. The 94.9% of the calculated results using the new heat transfer correlation were within ±30% of the experimental results.

Declaration of competing interest

The authors declare that they have no known competing financial interests or personal relationships that could have appeared to influence the work reported in this paper.

References

[1] Y.M. Li, J.S. Liaw, C.C. Wang, A criterion of heat transfer deterioration for supercritical organic fluids flowing upward and its heat transfer correlation, Energies 13 (2020), https://doi.org/10.3390/en13040989.
[2] D.E. Kim, M.H. Kim, Experimental investigation of heat transfer in vertical upward and downward supercritical CO2 flow in a circular tube, Int. J. Heat Fluid Flow 32 (2011) 176–191, https://doi.org/10.1016/j.ijheatfluidflow.2010.09.001.
[3] Y.Y. Bae, H.Y. Kim, D.J. Kang, Forced and mixed convection heat transfer to supercritical CO2 vertically flowing in a uniformly-heated circular tube, Exp. Therm. Fluid Sci. 34 (2010) 1295–1308, https://doi.org/10.1016/j.expthermflusci.2010.06.001.
[4] D.E. Kim, M.H. Kim, Two layer heat transfer model for supercritical fluid flow in a vertical tube, J. Supercrit. Fluids 58 (2011) 15–25, https://doi.org/10.1016/j.supflu.2011.04.014.
[5] Y. Huang, S. Liu, G. Liu, J. Wang, Y. Zan, X. Lang, Evaluation and analysis of forced convection heat transfer correlations for supercritical carbon dioxide in tubes, Nucl. Power Eng. 37 (2016) 28–33, https://doi.org/10.13832/j.jnpe.2016.01.0028.
[6] S. Liu, Y. Huang, Evaluation and analysis of forced convection heat transfer correlations for supercritical carbon dioxide in vertical tubes, in: H. Jiang (Ed.), Proc. 20th Pacific Basin Nucl. Conf., Singapore: Springer Singapore, 2017, pp. 753–768.
[7] S. Zhang, X. Xu, C. Liu, X. Liu, C. Dang, Experimental investigation on the heat transfer characteristics of supercritical CO2 at various mass flow rates in heated vertical-flow tube, Appl. Therm. Eng. (2019), https://doi.org/10.1016/j.applthermaleng.2019.04.097.
[8] H. Zhang, J. Xu, X. Zhu, J. Xie, M. Li, B. Zhu, The K number, a new analogy criterion number to connect pressure drop and heat transfer of sCO2 in

vertical tubes, Appl. Therm. Eng. 182 (2021) 116078, https://doi.org/10.1016/j.applthermaleng.2020.116078.
[9] S.M. Liao, T.S. Zhao, An experimental investigation of convection heat transfer to supercritical carbon dioxide in miniature tubes, Int. J. Heat Mass Tran. 45 (2002) 5025–5034, https://doi.org/10.1016/S0017-9310(02)00206-5.
[10] K. Tanimizu, R. Sadr, Experimental investigation of buoyancy effects on convection heat transfer of supercritical CO2 flow in a horizontal tube, Heat Mass Transf Und Stoffuebertragung 52 (2016) 713–726, https://doi.org/10.1007/s00231-015-1580-9.
[11] J. Wang, Z. Guan, H. Gurgenci, K. Hooman, A. Veeraragavan, X. Kang, Computational investigations of heat transfer to supercritical CO2 in a large horizontal tube, Energy Convers. Manag. 157 (2018) 536–548, https://doi.org/10.1016/j.enconman.2017.12.046.
[12] G.A. Adebiyi, W.B. Hall, Experimental investigation of heat transfer to supercritical pressure carbon dioxide in a horizontal pipe, Int. J. Heat Mass Tran. 19 (1976) 715–720, https://doi.org/10.1016/0017-9310(76)90123-X.
[13] Z. Zhao, B. Yuan, W. Du, Assessment and modification of buoyancy criteria for supercritical pressure CO2 convection heat transfer in a horizontal tube, Appl. Therm. Eng. 169 (2020) 114808, https://doi.org/10.1016/j.applthermaleng.2019.114808.
[14] E.W. Lemmon, M. Huber, M.O. Mclinden, E.W. Lemmon, M.L. Huber, O.M. Mclinden, NIST Standard Reference Database 23: Reference Fluid Thermodynamic and Transport Properties REFPROP 9.1.[DS], NIST NSRDS, 2010.
[15] T.H. Kim, J.G. Kwon, M.H. Kim, H.S. Park, Experimental investigation on validity of buoyancy parameters to heat transfer of CO2 at supercritical pressures in a horizontal tube, Exp. Therm. Fluid Sci. 92 (2018) 222–230, https://doi.org/10.1016/j.expthermflusci.2017.11.024.
[16] V. Nieolinski, New equations for heat mass transfer in turbulent pipe and channel flows, Int. Chem. Eng. 16 (1976) 359–368.
[17] R.J. Moffat, Describing the uncertainties in experimental results, Exp. Therm. Fluid Sci. 1 (1988) 3–17, https://doi.org/10.1016/0894-1777(88)90043-X.
[18] J.D. Jackson, Fluid flow and convective heat transfer to fluids at supercritical pressure, Nucl. Eng. Des. 264 (2013) 24–40, https://doi.org/10.1016/j.nucengdes.2012.09.040.
[19] D.M. McEligot, J.D. Jackson, "Deterioration" criteria for convective heat transfer in gas flow through non-circular ducts, Nucl. Eng. Des. 232 (2004) 327–333, https://doi.org/10.1016/j.nucengdes.2004.05.004.
[20] D.E. Kim, M.H. Kim, Experimental study of the effects of flow acceleration and buoyancy on heat transfer in a supercritical fluid flow in a circular tube, Nucl. Eng. Des. 240 (2010) 3336–3349, https://doi.org/10.1016/j.nucengdes.2010.07.002.
[21] F.W. Dittus, L.M.K. Boelter, Heat transfer in automobile radiators of the tubular type, Int. Commun. Heat Mass Tran. 12 (1985) 3–22, https://doi.org/10.1016/0735-1933(85)90003-X.
[22] V.A. Kurganov, Y.A. Zeigarnik, I.V. Maslakova, Heat transfer and hydraulic resistance of supercritical pressure coolants. Part III: generalized description of SCP fluids normal heat transfer, empirical calculating correlations, integral method of theoretical calculations, Int. J. Heat Mass Tran. 67 (2013) 535–547, https://doi.org/10.1016/j.ijheatmasstransfer.2013.07.056.
[23] J.D. Jackson, An semi-empirical model of turbulent convective heat transfer to fluids at supercritical pressure, in: Proc. 16th Int. Conf. Nucl. Eng vol. 3, 2008, pp. 911–921, https://doi.org/10.1115/ICONE16-48914. Orlando, Florida, USA.
[24] H. Li, A. Kruizenga, M. Anderson, M. Corradini, Y. Luo, H. Wang, et al., Development of a new forced convection heat transfer correlation for CO2 in both heating and cooling modes at supercritical pressures, Int. J. Therm. Sci. 50 (2011) 2430–2442, https://doi.org/10.1016/j.ijthermalsci.2011.07.004.